

Suppressing flow-induced vibration of HGA by an acoustic PZT actuator in hard disk drives

Guoqing Zhang¹ · Yun Yang¹ · Hui Li¹ · Shengnan Shen¹ · Shijing Wu¹

Received: 19 September 2015 / Accepted: 9 December 2015 / Published online: 21 December 2015
© Springer-Verlag Berlin Heidelberg 2015

Abstract The reliability and stability of hard disk drives (HDDs) is especially important as the areal recording density increasing rapidly target to 10 Tb/in² in the future. The vibration of the Head Gimbals Assembly (HGA) is inevitable by internal fluid flow during operational process. In order to improve this undesirable problem, an acoustic piezoelectric transducer (PZT) actuator which can be used to transform an electric current to an acoustic pressure field, is glued on the HDD cover inner surface to generate acoustic pressure to suppress the flow-induced off-plate vibration (FIOPV) of the HGA. In this paper, a three-dimensional finite element model of HDD is built with an acoustic PZT actuator. The FIOPV of the HGA in the air and helium-filled drives are investigated by fluid–structure interaction simulation method. The acoustic pressure induced vibration (APIV) of the HGA is analyzed by acoustics-piezoelectric-structure interaction simulation method. After that, the suppressed FIOPV after superposing the APIV and the FIOPV is obtained by following the superposition principle.

1 Introduction

In recent years, the areal recording density of hard disk drives (HDDs) is increasing rapidly for the continual demand of mass storage, which requires ultra-low flying height, more accurate seeking position, and higher disk rotation speed. However, the high speed rotary flow inside the narrow HDDs space inevitably induces vibrations on

the Head Gimbals Assembly (HGA), which may lead to some undesirable problems, such as positioning error or even devastating head-disk crash. In order to enhancing the robustness of drives in the operational process, it is very important to mitigate the flow-induced off-plate vibration (FIOPV) on the HGA. Some previous works have been focused on the flow-induced vibration issues inside the drives (Ikegawa et al. 2006; Ng et al. 2011; Shimizu et al. 2003; Tsuda et al. 2003; Aruga et al. 2007; Zhang et al. 2010), including mechanism analysis and structure optimization studies of the vibrations. However, they were passive methods to alleviate the vibrations and would not be controllable due to different fluid fields inside the drives. Recently, Min et al. (2012a, b, 2013a, b, c, 2014a, b) systematically studied the relationship between the flow pressure fluctuations around the HGA and the vibrations of the HGA. They introduced a piezoelectric transducer (PZT) which can be used to transform an electric current to an acoustic pressure field, glued onto the inner surface of the HDD cover to generate acoustic pressure to suppress the HGA flow-induced vibration in their experiments. Their results provided a new method to use acoustic pressure to balance the flow pressure fluctuations. However, there exist some deficiencies in their work. Due to the hole drilled on the drive cover and the slot cut on the side base, the flow field around the HGA may have changed. In addition, the 2-D model they used cannot truly represent the real 3-D flow field inside the HDD, and the pressure redistribution is not clear due to the introduced PZT. Moreover, the experimental investigations are hardly carried out to study the helium-filled HDDs by the similar method because of the difficulty of tight seal (Kil et al. 2012a, b). Yet till now, there are no simulation results in mitigating the vibrations of the HGA inside air-filled and helium-filled drives by the introduced acoustic pressure method.

✉ Hui Li
li_hui@whu.edu.cn

¹ School of Power and Mechanical Engineering, Wuhan University, Wuhan 430072, China

In this paper, the flow-induced off-plate vibration (FIOPV) of the HGA and its suppression by an acoustic PZT actuator in the air-filled and helium-filled drives are studied respectively, using the fluid–structure and acoustics–piezoelectric–structure interaction simulation method. Firstly, a three-dimensional finite element model of HDD is built with an acoustic PZT actuator. Then, the flow-induced vibration spectrum of the HGA is analyzed using the fast Fourier transform algorithm. After that, by designing an acoustic PZT actuator on the HDD cover inner surface, the acoustic pressure induced vibration (APIV) of the HGA is analyzed. Finally, the suppressed vibration after superposing APIV and FIOPV is obtained by following the superposition principle.

2 Methodology

A geometrical model of a 2.5-inch HDD with the HGA positioned at the middle diameter, which was built by our previous work (Zhang et al. 2015), is shown in Fig. 1. The length of the slider is 0.85 mm and its width and height are 0.70 and 0.23 mm, respectively. The initial gap between slider and disk is 0.17 mm. The disk is rotated at 10,000 rpm. An acoustic PZT actuator with a diameter of 20 mm and thickness of 1 mm was designed on the HDD cover inner surface as shown in Fig. 1b. The investigated filling gases in the HDD include air and helium, and their physical properties are listed in Table 1.

The suppression of the FIOPV of the HGA in this work is a typical multi-physics filed interaction issue involving fluid–structure interaction (FSI) and acoustics–piezoelectric–structure interaction. The commercial software ANSYS 15.0 (ANSYS Inc. 2013) is used to perform the simulation. The material properties of the drive model are presented in Table 2. Due to the complexity of the HDD geometry and the interaction simulation, the work is divided into three parts: (1) FSI analysis to obtain the FIOPV; (2) acoustics–piezoelectric–structure interaction analysis to study the APIV; (3) superposition of the FIOPV and APIV.

Part 1 Computational fluid dynamics (CFD) simulation is carried out to calculate the aerodynamic forces acting on the arm and the HGA. In order to simulate the flow perturbations accurately, the large eddy simulation (LES) model is used (Zhang et al. 2010). The important parameters including mesh size, mesh quantity, y^+ and time step should be properly valued before performing LES simulation. In our simulation, the Kolmogorov length scale $\eta = 0.026$ mm is calculated by

$$\eta = \left(\frac{\nu^3}{\varepsilon} \right)^{1/4} \quad (1)$$

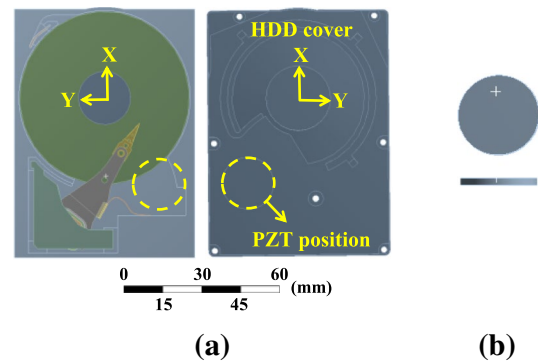


Fig. 1 **a** Geometric model of a 2.5-inch HDD and **b** acoustic PZT actuator

Table 1 Physical properties of air and helium used in this work

Properties	Air	Helium
Mass density ρ : (kg/m ³)	1.251	0.179
Kinematic viscosity: ν (m ² /s)	1.38×10^{-5}	1.02×10^{-4}
Sound speed: (m/s)	343	923

where ν is the kinematic viscosity, ε is the turbulent dissipation rate. The mesh size near the HGA we used is 0.05 mm which is about twice of the Kolmogorov length scale. In addition, there are at least three nodes in the shortest edge. The time step for the CFD simulation is set to 10 μ s, which is about one-fifth of the Kolmogorov time scale $\tau_\eta = 51$ μ s calculated by

$$\tau_\eta = \left(\frac{\nu^3}{\varepsilon} \right)^{1/2} \quad (2)$$

The equiangle skew of grid cells near the HGA, Q_{EAS} , ranges from 0 to 0.35 calculated by

$$Q_{EAS} = \max \left\{ \frac{\theta_{max} - \theta_e}{180 - \theta_e}, \frac{\theta_e - \theta_{min}}{\theta_e} \right\} \quad (3)$$

where, θ_{max} and θ_{min} are the maximum and minimum angles between the edges of the mesh element, and θ_e is the characteristic angle corresponding to an equilateral cell of similar form. Boundary layer mesh on surfaces is constructed. The y^+ of the near-wall mesh cell is reasonable. Therefore, the LES model is considered acceptable in our simulation.

The RNG $k - \varepsilon$ turbulent model is performed for the air flow in steady state simulation, while the laminar model is used for the helium flow (Aruga et al. 2007). Then, the LES method is carried out for the transient simulation, and the subgrid-scale flow structures are modeled using a dynamic adaptation of the Smogorinsky-Lilly model (Kazemi 2008). The spatial and time derivatives are approximated using bounded central-differencing and second order upwind

Table 2 Material properties used in this work

Component	Materials	Density (kg/m ³)	Young’s modulus (GPa)	Poisson’s ration
Base/motor	Aluminum	2719	70	0.33
Bobbin	ABS	1130	3.2	0.30
Coil	Copper	8978	117	0.34
Arm/suspension	Stainless steel	7930	193	0.30
Slider	TiC	4940	450	0.18
Disk	Glass	2700	69	0.33
Magnet	FeNiCo	4560	54.3	0.30

discretization schemes. The transient computations are executed for 50 ms so as to allow flow reach to statistically steady. Thereafter, the aerodynamic forces are collected for 200 ms to conduct the subsequent structure vibration analysis. The spectrum of FIOPV is calculated with the fast Fourier transform algorithm.

Part 2 PZT-5H which has good piezoelectric properties is chosen as an acoustic pressure exciting source in this work. Its material properties are as follows:

$$[\varepsilon] = \begin{bmatrix} 1.503 & 0 & 0 \\ 0 & 1.503 & 0 \\ 0 & 0 & 13 \end{bmatrix} 10^{-8} \text{ (F/m)}$$

$$[c] = \begin{bmatrix} 127.21 & 80.20 & 84.67 & 0 & 0 & 0 \\ 0 & 127.20 & 84.67 & 0 & 0 & 0 \\ 0 & 0 & 117.44 & 0 & 0 & 0 \\ 0 & 0 & 0 & 22.99 & 0 & 0 \\ 0 & 0 & 0 & 0 & 22.99 & 0 \\ 0 & 0 & 0 & 0 & 0 & 23.47 \end{bmatrix} \text{ (GPa)}$$

$$[e] = \begin{bmatrix} 0 & 0 & 0 & 0 & 17 & 0 \\ 0 & 0 & 0 & 17 & 0 & 0 \\ -6.5 & -6.5 & 23.3 & 0 & 0 & 0 \end{bmatrix} \text{ (C/m}^2\text{)}$$

where $[\varepsilon]$ is the dielectric constant matrix, $[c]$ is the elastic coefficient matrix, and $[e]$ is the piezoelectric stress matrix. The density of PZT-5H is 7600 kg/m³ and the Poisson’s ratio is 0.28.

The acoustics-piezoelectric-structure interaction in this work comprises three fundamental physics: acoustic pressure, solid mechanics and electrostatics. The wave equations for sound propagation in the HDD filling with gas medium can be described by an equation in the Cartesian coordinate systems as (Yi et al. 2001):

$$\nabla^2 p(x, t) - \frac{1}{c^2} \cdot \frac{\partial^2 p(x, t)}{\partial t^2} \tag{4}$$

where ∇ is the Laplace operator, p denotes the acoustic pressure in terms of the receiver position x and time t , and c represents the speed of acoustic wave in the gas medium. The acoustic speed in air and helium are taken as 343 and 923 m/s as listed in Table 1. While the maximum speeds

of air flow and helium flow are much <1 Mach at the disk rotation speed of 10,000 RPM, therefore c can be assumed to equal the value in the static flow (Min et al. 2013a).

The solid mechanics and electrostatics physics are coupled via the constitutive equations that correlate stresses and strains to electric displacement and electric field. These physics interfaces solve for the balance of body forces σ and volume charge density D respectively as shown in Eqs. (5) and (6):

$$\nabla \cdot \sigma = 0 \tag{5}$$

$$\nabla \cdot D = 0 \tag{6}$$

At the interface between the gas medium and solid domain, the normal acceleration of the solid (PZT) surface is used to drive the gas domain. This is described by the following equation:

$$n \cdot \left(\frac{1}{\rho} (\nabla p) \right) = a_n \tag{7}$$

where n is denotes the normal direction, ρ is the density of medium, a_n is the normal acceleration.

The acoustic pressure at the interface between the gas medium and solid domain acts as a boundary load on the solid:

$$n \cdot \sigma = p \tag{8}$$

The boundaries of the cover inner surface, disk surface and HGA surfaces are assumed to be acoustically rigid for the acoustic field.

Part 3 In structural analysis, the motion of HGA induced by flow pressure fluctuations can be described as linear vibration (Liu et al. 2011). From this, the motion of HGA induced by acoustic pressure oscillations can be considered to be linear vibration (Min et al. 2013a). These vibrations can be divided into a number of harmonic vibrations. Based on the vibration theory, the superposition principle can be applied in linear vibration system. The APIV of up suspension tip is calculated in the static flow in the harmonic response simulation. And then, the total vibration x of up suspension tip after suppressing is obtained by superposing the only APIV and the only FIOPV, which can be written as:

$$x = x_1 + x_2 \tag{9}$$

$$x_1 = A_1 \cdot \cos(\omega t + \varphi_1) \tag{10}$$

$$x_2 = A_2 \cdot \cos(\omega t + \varphi_2) \tag{11}$$

where A_i is the vibration amplitude, ω is the vibration frequency, φ_i is the vibration phase, and subscripts 1 and 2 denote the APIV and FIOPV, respectively. The total vibration can be rewritten as:

$$x = A_1 \cdot \cos(\omega t + \varphi_1) + A_2 \cdot \cos(\omega t + \varphi_2) = A \cdot \cos(\omega t + \varphi) \tag{12}$$

where

$$A^2 = A_1^2 + A_2^2 + 2A_1A_2\cos(\varphi_2 - \varphi_1) \tag{13}$$

$$\tan\varphi = \frac{A_1\sin\varphi_1 + A_2\sin\varphi_2}{A_1\cos\varphi_1 + A_2\cos\varphi_2} \tag{14}$$

The PZT exciting voltage amplitude and phase are denoted by A_3 and φ_3 , respectively. From Eq. (13), the phase difference between the APIV and FIOPV should be 180° , thus $\cos(\varphi_2 - \varphi_1) = -1$, to achieve a good suppression on the vibration of the up suspension tip. That is,

$$|\varphi_2 - \varphi_1| = 180 \tag{15}$$

Since the FIOPV phase φ_2 is already obtained in part 1, the required APIV phase φ_1 can be easily calculated. In turn, the required PZT exciting voltage (A_3, φ_3) can be decided, since the PZT exciting voltage is the source of above APIV.

Considering the extreme complexity of multi-physics filed interaction involving fluid–structure-acoustics-piezoelectric, in this simulation, the suppressed vibration of up suspension tip is calculated by superposing the only FIOPV and the only APIV, since the flow field has no obvious effects on the acoustic field in HDD at disk rotation speed of 10,000 rpm (Min et al. 2013a). In details, firstly, we calculate the flow-induced off-plate vibration of HGA, to find out the principal frequencies where large vibration amplitudes appear. Secondly, it tries to design proper PZT exciting voltage amplitude and phase, to efficiently suppress the peak vibration amplitudes at above principal frequencies. Finally, it calculates the superposition of above obtained APIV and FIOPV.

3 Results and discussion

3.1 Flow-induced vibration of HGA

In the structure vibration analysis of FSI, the timestep is set to 20 μ s, which corresponds to a Nyquist frequency of

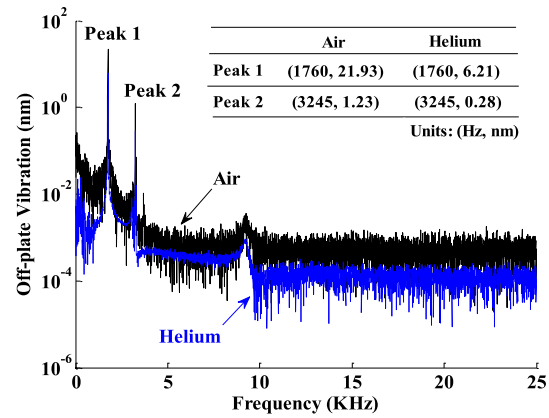


Fig. 2 Off-plate vibration of up suspension tip induced by flow versus frequency

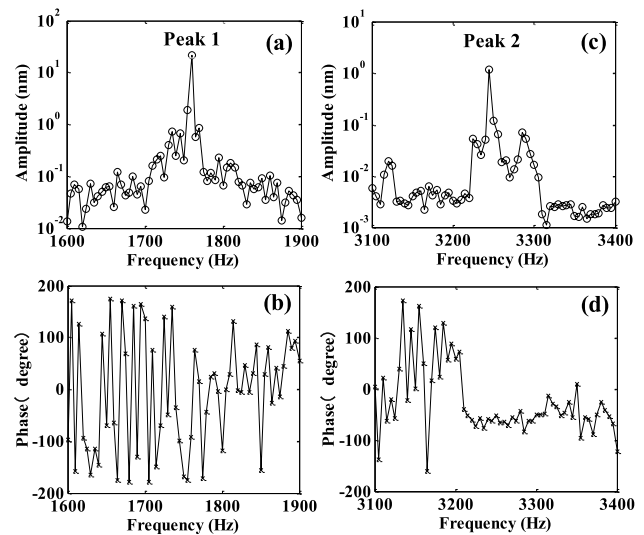


Fig. 3 Spectra of up suspension tip off-plate vibration only induced by air flow at a, b 1760 Hz and c, d 3245 Hz in the air-filled drive

25 kHz. Figure 2 shows the FIOPV of up suspension tip as a function of frequency. It can be seen that the spectrum appears two principal frequencies named as peak1 (1760 Hz) and peak2 (3245 Hz) in the both air and helium-filled drives. Moreover, the first principal frequency (1760 Hz) which has the maximum vibration amplitude is almost the same as the 1st natural frequency 1759 Hz of arm-suspension. It means that the first mode (1st bending mode) of arm-suspension dominates the FIOPV of the HGA. Figures 3 and 4 show the bode plot of the FIOPV spectrum of up suspension tip at 1760 and 3245 Hz in the drives filling with air and helium, respectively. The corresponding FIOPV amplitudes and phases are listed in Table 3.

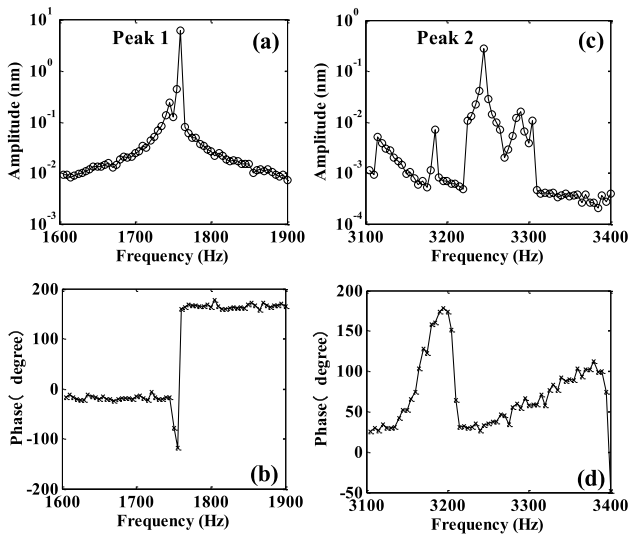


Fig. 4 Spectra of up suspension off-plate vibration tip only induced by helium flow at **a, b** 1760 Hz and **c, d** 3245 Hz in the helium-filled drive

Table 3 The flow-induced off-plate vibration of up suspension tip

Principal frequency	(Amplitude: A_2 , phase: φ_2) (unit: nm, °)	
	Air-filled drive	Helium-filled drive
Peak 1 (1760 Hz)	(21.93, -92.44)	(6.21, 160.17)
Peak 2 (3245 Hz)	(1.23, -59.86)	(0.28, 33.51)

3.2 Acoustic pressure induced vibration of HGA

To improve the flying head stability, it is necessary to suppress the FIOPV, especially the peak amplitudes at two principal frequencies as shown in Fig. 2. Harmonic response analyses are conducted to find out the proper PZT exciting voltage amplitude A_3 and phase φ_3 , which can efficiently suppress the peak vibration amplitudes at above two principal frequencies of FIOPV.

Figure 5 shows the APIV amplitude A_1 and the phase φ_1 of the up suspension tip at 1760 Hz as a function of the PZT exciting voltage amplitude A_3 with the phase $\varphi_3 = 0$ degree. It can be obviously seen that the APIV amplitude A_1 of the up suspension tip is directly proportional to the PZT exciting voltage amplitude A_3 .

Figure 6 also shows a directly proportional relationship between PZT exciting voltage phase φ_3 and resultant APIV phase φ_1 of the up suspension tip at 1760 Hz when the PZT exciting voltage amplitude A_3 chosen as 100 V. And the difference between the PZT exciting voltage phase φ_3 and the APIV phase φ_1 is always 178.33, that is, $\varphi_3 - \varphi_1 = 178.33$ degree.

According to the discussion in part 3 of methodology section and Eq. (15), it can get $\varphi_3 - \varphi_2 = (\varphi_3 - \varphi_1) - |\varphi_2 - \varphi_1| = 178.33 - 180 = -1.67$ degree. Due to the FIOPV

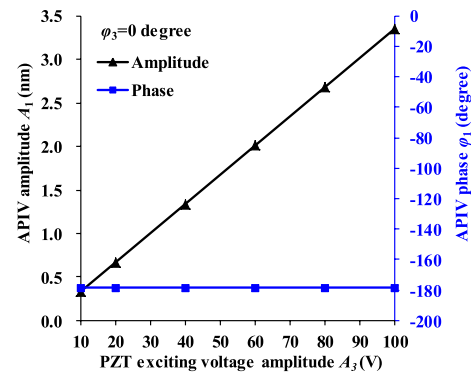


Fig. 5 The APIV amplitude A_1 and phase φ_1 of up suspension tip at 1760 Hz versus PZT exciting voltage amplitude A_3 ($\varphi_3 = 0$) in the air-filled drive

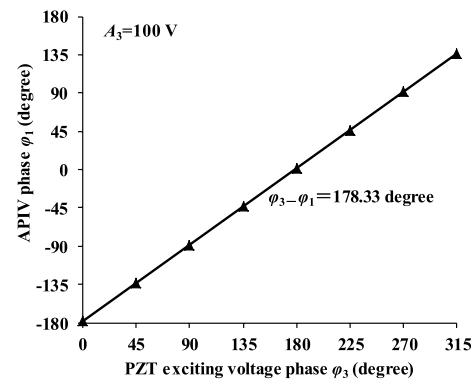


Fig. 6 The APIV phase φ_1 of up suspension tip at 1760 Hz versus PZT exciting voltage phase φ_3 ($A_3 = 100$ V) in the air-filled drive

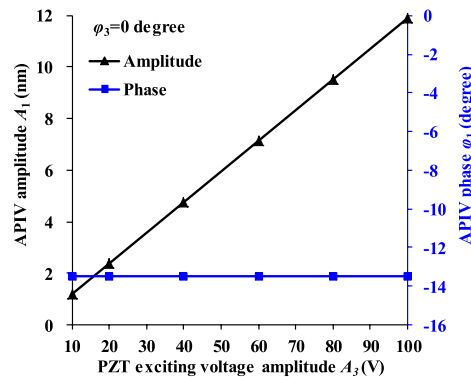


Fig. 7 The APIV amplitude A_1 and phase φ_1 of up suspension tip at 3245 Hz versus PZT exciting voltage amplitude A_3 ($\varphi_3 = 0$) in the air-filled drive

phase φ_2 is -92.44 degree as listed in Table 3, the required PZT exciting voltage phase φ_3 is calculated and its value equals to -94.11 degree when the PZT exciting voltage amplitude A_3 chosen as 100 V.

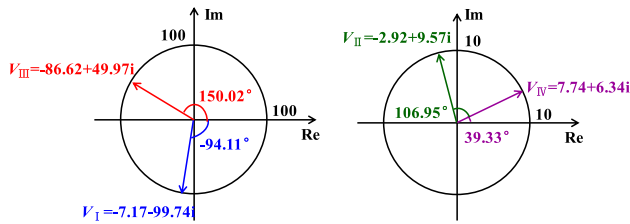


Fig. 8 The calculated PZT exciting voltage for suppressing the peak amplitudes at two principal frequencies of FIOPV in Figs. 3 and 4

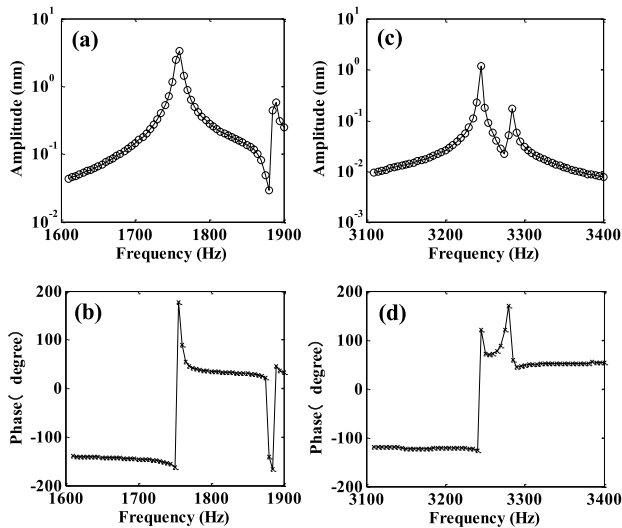


Fig. 9 Spectra of up suspension tip off-plate vibration only induced by PZT generating acoustic pressure at a, b 1760 Hz and c, d 3245 Hz in the air-filled drive

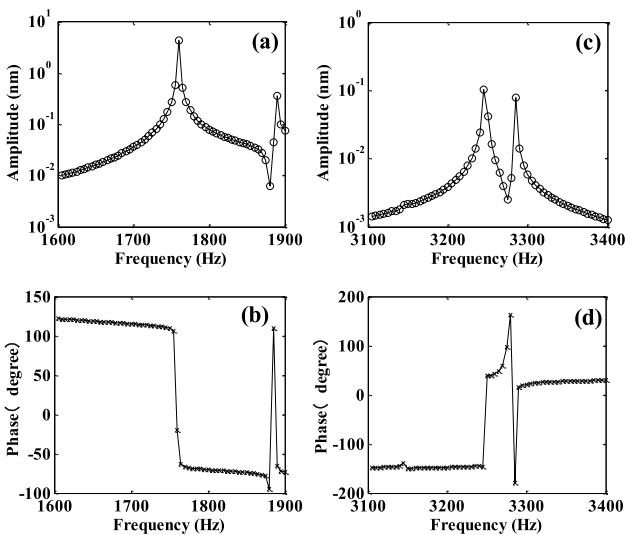


Fig. 10 Spectra of up suspension tip off-plate vibration only induced by PZT generating acoustic pressure at a, b 1760 Hz and c, d 3245 Hz in the helium-filled drive

Table 4 The acoustic pressure induced off-plate vibration of up suspension tip

Principal frequency	(Amplitude: A_1 , phase: φ_1) (unit: nm, degree)	
	Air-filled drive	Helium-filled drive
Peak 1 (1760 Hz)	(3.35, 87.56)	(4.31, -19.83)
Peak 2 (3245 Hz)	(1.19, 120.14)	(0.10, -146.49)

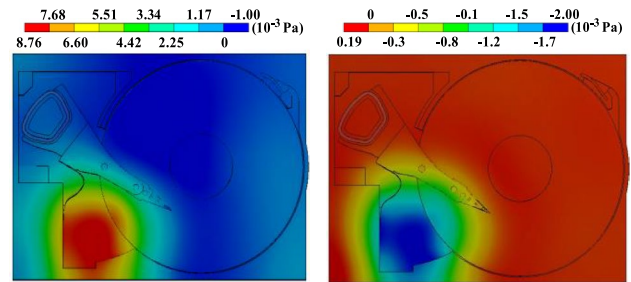


Fig. 11 Acoustic pressure distribution in the air-filled drive at the frequencies of a 1760 Hz and b 3245 Hz

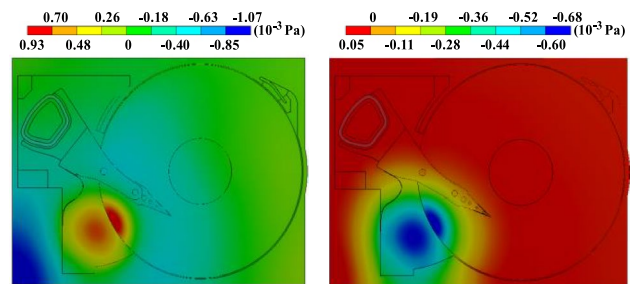


Fig. 12 Acoustic pressure distribution in the helium-filled drive at the frequencies of a 1760 Hz and b 3245 Hz

Figure 7 shows that at the second principal frequency of 3245 Hz, the APIV amplitude can achieve 1.19 nm when the PZT exciting voltage A_3 chosen as 10 V. It can be found that the difference between the PZT exciting voltage phase φ_3 and the APIV phase φ_1 is -13.19 at 3245 Hz, that is, $\varphi_3 - \varphi_1 = -13.19$ degree. According to the discussion in part 3 of methodology section and Eq. (15), it can get $\varphi_3 - \varphi_2 = (\varphi_3 - \varphi_1) - |\varphi_2 - \varphi_1| = -13.19 - (-180) = 166.81$ degree. Due to the FIOPV phase φ_2 is -59.86 degree as listed in Table 3, the required PZT exciting voltage phase φ_3 is obtained as 106.95 degree when the PZT exciting voltage amplitude A_3 chosen as 10 V, as shown in Fig. 8.

Similarly, the required PZT exciting voltage amplitude A_3 and phase φ_3 in the helium-filled drive are obtained as shown in Fig. 8. V_I and V_{II} are used for the air-filled HDD, while V_{III} and V_{IV} are used for the helium-filled HDD. The corresponding APIV spectrum of the up suspension tip induced by above four PZT exciting voltages are shown in

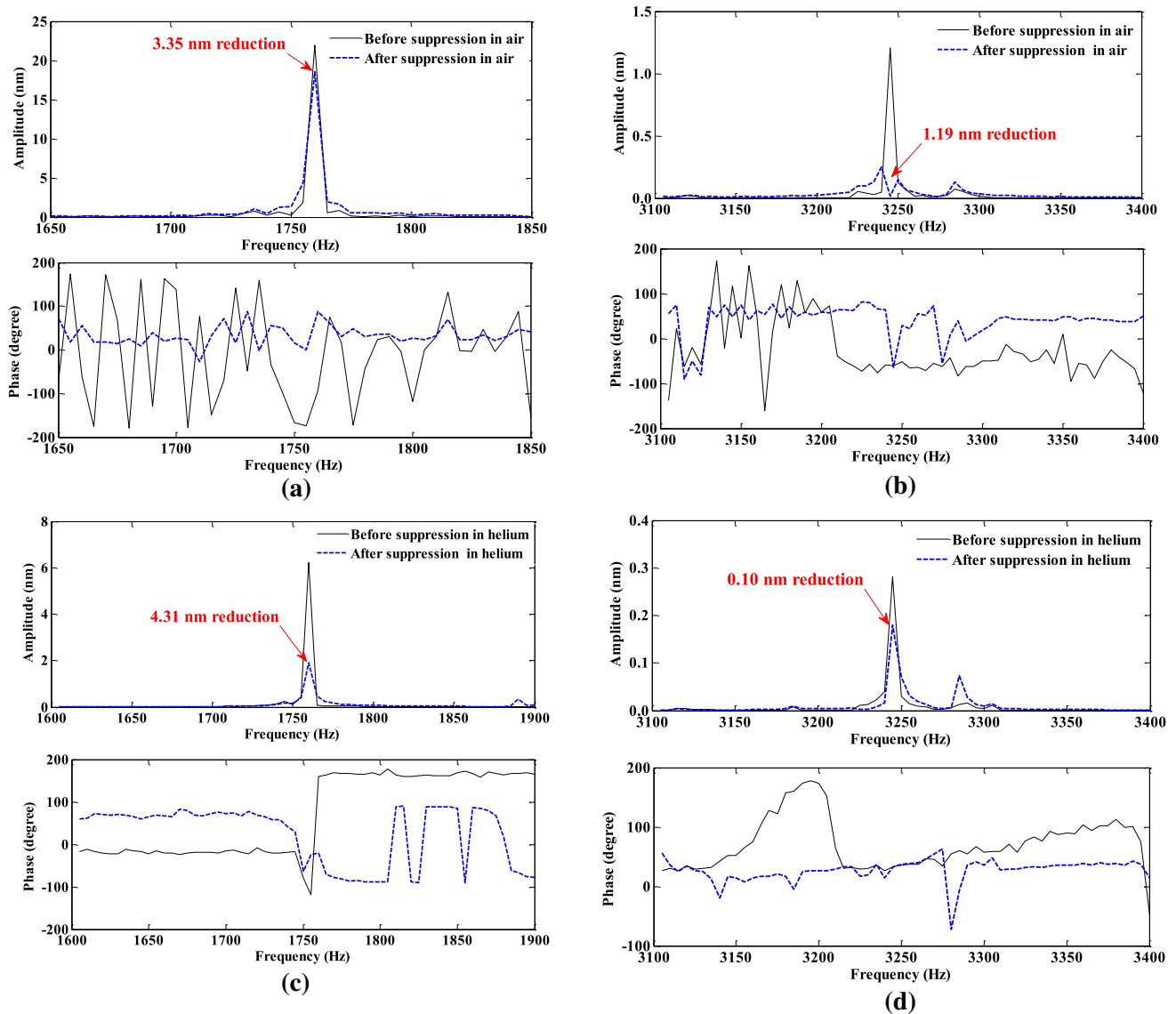


Fig. 13 Spectra of up suspension tip off-plate vibration before and after introducing acoustic PZT actuator in the **a, b** air-filled and **c, d** helium-filled drives

Figs. 9 and 10. The corresponding APIV amplitudes and phases are summarized in Table 4.

Figure 11 shows the acoustic pressure distribution in the air-filled drive at 1760 and 3245 Hz. It can be seen that the pressure value at 1760 Hz is much bigger than that at 3245 Hz. Figure 12 shows the acoustic pressure distribution in the helium-filled drive at 1760 and 3245 Hz, respectively, and its maximum value at 3245 Hz is much smaller.

3.3 The superposition of FIOPV and APIV

The superposition of APIV (x_1) and FIOPV (x_2) can be obtained according to the Eqs. (12–14) by following the

superposition principle. The superposition results of up suspension tip vibration (x) at two principal frequencies are presented in Fig. 13.

From Fig. 13a, it shows that a suppression up to 3.35 nm (15.3 %) of peak amplitude is achieved at 1760 Hz in the air-filled drive. Figure 13b shows that there is a 1.19 nm (96.7 %) reduction of peak amplitude at 3245 Hz in the air-filled drive. And the phases after superposition are obviously changed.

By conducting the superposition in the helium-filled drive (Fig. 13c, d), a suppression up to 4.31 (69.4 %) and 0.10 nm (35.7 %) of peak amplitude is obtained, respectively.

4 Summary

In this paper, a three-dimensional finite element model of hard disk drive (HDD) is built with an acoustic PZT actuator, which is glued on the cover inner surface of the HDD to generate acoustic pressure to suppress the flow-induced off-plate vibration of the HGA. The voltage amplitude 100 and 10 V are used as the PZT exciting voltages for suppressing the peaks amplitude at 1760 and 3245 Hz in the flow-induced off-plate vibration spectrum, respectively.

It indicates that it is effective to suppress the FIOPV by an acoustic PZT actuator. The results show that distinct suppression can be achieved at two principal frequencies. For suppressing the peak amplitude at 1760 Hz in the air-filled drive, a distinct reduction of 3.35 nm (15.3 %) is obtained, while the suppression at 3245 Hz is about 1.19 nm (96.7 %). For the suppression in the helium-filled drive, suppression up to 4.31 (69.4 %) and 0.10 (35.7 %) nm can be obtained at 1760 and 3245 Hz, respectively.

Acknowledgments This work is supported by National Natural Science Foundation of China (Grant No. 51505342), and the Fundamental Research Funds for the Central Universities of China (Grant No. 2042015kf0193).

References

- ANSYS Inc. (2013) ANSYS v15.0. Available: <http://www.ansys.com/>
- Aruga K, Suwa M, Shimizu K, Watanabe T (2007) A study on positioning error caused by flow induced vibration using helium-filled hard disk drives. *IEEE Trans Magn* 43:3750–3755
- Ikegawa M, Hirono Y, Mukai H, Kaiho M (2006) Decreasing airflow velocity in hard disk drives with a spoiler and bypass. *IEEE Trans Magn* 42:2594–2596
- Kazemi M (2008) Analysis of the slider off-track vibration caused by the aerodynamic loads associated with different components of a head stack assembly in a disk drive. *IEEE Trans Magn* 44:633–639
- Kil SW, Humphrey JAC, Haj-Hariri H (2012a) Numerical study of the flow-structure interactions in an air- or helium-filled simulated hard disk drive. *Microsyst Technol* 18:57–75
- Kil SW, Humphrey JAC, Haj-Hariri H (2012b) Experimental study of the flow-structure interactions in an air- or helium-filled hard disk drive geometry. *Microsyst Technol* 18:43–56
- Liu NY, Zhang QD, Sundaravadivelu K (2011) A new fluid structure coupling approach for high frequency/small deformation engineering application. *IEEE Trans Magn* 47:1886–1889
- Min H, Huang X, Zhang QD (2012a) Aerodynamic pressure fluctuations associated with flow-induced vibration of the head gimbals assembly inside a hard disk drive. *IEEE Trans Magn* 48:101–106
- Min H, Huang X, Zhang QD (2012b) Pressure fluctuations and flow-induced vibration measurements in a hard disk drive under different rotation speeds. *Appl Mech Mater* 197:292–296
- Min H, Huang X, Zhang QD (2013a) Active control of flow-induced vibrations on slider in hard disk drives by suppressing pressure fluctuations with virtual sensing. *IEEE Trans Magn* 49:1088–1095
- Min H, Huang X, Zhang QD (2013b) Active control of flow-induced vibrations on slider in hard disk drives: experimental demonstration. *IEEE Trans Magn* 49:3038–3041
- Min H, Huang X, Zhang QD (2013c) Active control on flow-induced vibration of the head gimbals assembly in hard disk drives. *IEEE Trans Magn* 49:2653–2656
- Min H, Huang X, Zhang QD (2014a) Narrowband performance of active control on flow-induced vibrations inside hard disk drives. *Microsyst Technol* 20:1557–1563
- Min H, Huang X, Zhang QD (2014b) Digital feedback control of the flow-induced vibrations on the head gimbals assembly in hard disk drives: design and implementation. *IEEE Trans Magn* 50:3302106
- Ng EYK, Liu NY, Tan YCM (2011) Structure optimization study of hard disk drives to reduce flow-induced vibration. *Open Numer Methods J* 3:31–41
- Shimizu H, Shimizu T, Tokuyama M, Masuda H, Nakamura S (2003) Numerical simulation of positioning error caused by air-flow-induced vibration of head gimbal assembly in hard disk drive. *IEEE Trans Magn* 39:806–811
- Tsuda N, Kubotera H, Tatewaki M, Noda S, Hashiguchi M, Maruyama T (2003) Unsteady analysis and experimental verification of the aerodynamic vibration mechanism of HDD arms. *IEEE Trans Magn* 39:819–825
- Yi S, Ling SF, Ying M (2001) Time-domain analyses of acoustics-structure interactions for piezoelectric transducers. *J Acoust Soc Am* 109:2762–2770
- Zhang QD, Tan CS, Sundaravadivelu K, Suriadi MA, Chin GL, Yip TH, Ong EH, Liu NY (2010) Mitigation of flow induced vibration of head gimbal assembly. *Microsyst Technol* 16:213–219
- Zhang GQ, Li H, Shen SN, Lei J, Zheng H, Wu SJ (2015) Simulation of temperature around laser-heating media in heat-assisted magnetic recording. *Microsyst Technol*. doi:10.1007/s00542-015-2654-9